

April 2014

Rational Curves and $(0,2)$ -Deformations

Paul S. Aspinwall and Benjamin Gaines

Department of Mathematics
Duke University, Durham, NC 27708-0320

Abstract

We compare the count of $(0,2)$ -deformation moduli fields for $N = (2,2)$ conformal field theories on orbifolds and sigma-models on resolutions of the orbifold. The latter involves counting deformations of the tangent sheaf. We see there is generally a discrepancy which is expected to be explained by worldsheet instanton corrections coming from rational curves in the orbifold resolution. We analyze the rational curves on the resolution to determine such corrections and discover that irreducible toric rational curves account for some, but not all, of the discrepancy. In particular, this proves that there must be worldsheet instanton corrections beyond those from smooth isolated rational curves.

arXiv:1404.7802v1 [hep-th] 30 Apr 2014

1 Introduction

Using comparisons between conformal field theory and geometry to predict facts about rational curves has been famously successful in the context of mirror symmetry [1]. In this paper we will make another such comparison which should be quite distinct as it lives outside the world of mirror symmetry and topological field theory.

Here we are concerned with (0,2)-superconformal field theories obtained from a non-linear σ -model associated to a Calabi-Yau threefold X equipped with a rank 3 holomorphic vector bundle $V \rightarrow X$. Let \mathcal{T} be the tangent bundle of X . We consider the case where the (0,2) superconformal field theory is a first order deformation of a (2,2) theory. Geometrically this means that V is a first order deformation of \mathcal{T} .

We will consider the case where X is a projective resolution of an orbifold \mathbb{C}^3/G and compare the number of deformations of the conformal field theory to the number of deformations of \mathcal{T} . Any discrepancy should be due to worldsheet instantons which probes the structure of rational curves in X .

The subject of worldsheet instanton corrections in non-linear σ -models has a fascinating history. They were first analyzed in the sequence of papers [2, 3]. Here it was realized that typically they could produce corrections to the superpotential resulting in one-point functions that would destabilize the vacuum. That is, the combination $V \rightarrow X$ could not be used for string compactifications.

The special case, where V is the tangent bundle \mathcal{T} , leads to (2,2) worldsheet supersymmetry. It is well-known that these give perfectly good string compactifications. Here the instantons do not destroy the vacuum but do correct certain three-point functions. Analysis of such corrections by using mirror symmetry to compare geometry and exact conformal field theory [1, 4] led to the present day flourishing of Gromov–Witten theory (see, for example, [5]).

Meanwhile it was realized that some other (0,2)-models might actually be okay too. If the bundle V is restricted to a rational curve $C \subset X$ then it will always split

$$V|_C = \mathcal{O}(a) \oplus \mathcal{O}(b) \oplus \mathcal{O}(c), \tag{1}$$

where $a + b + c = 0$, since $c_1(V) = 0$. In [6, 7] it was emphasized that, in the case of isolated (to first order) curves, instantons could only produce those dangerous one-point functions if V split “trivially”, i.e., $a = b = c = 0$. So if V splits nontrivially on *every* rational curve, the model is good. This explains why (2,2)-models are good, since $V \cong \mathcal{T}$ and adjunction implies $a \geq 2$. Unfortunately, as we review in appendix, $a = b = c = 0$ is the *generic* case for a bundle over \mathbb{P}^1 . Thus, unless there are global obstructions in X to prevent such a splitting, a generic deformation of V away from a (2,2)-model would seem to be bad. So generic $V \rightarrow X$ still tend to give invalid models.

There is another way of killing the instanton corrections. It may be that each rational curve gives a nonzero contribution to one-point functions, but these contributions magically cancel when all the rational curves are added up. Such a miracle indeed happens for the quintic threefold [8] as was explained further in [9]. The generic quintic has 2875 lines and

over each of these lines a generic deformation of \mathcal{S} will split trivially. However, such a deformation of \mathcal{S} always has zero net instanton corrections to one-point functions since the contribution from these lines cancel. Similarly all higher degree rational curves cancel too.

Because of this, (0,2)-models sometimes seem to be plagued by a contradiction: even though a generic model should be killed by instanton effects, anything you can actually write down (and, in particular, know the exact conformal field theory) probably isn't generic and is perfectly fine! More precisely, the analysis of [9] suggests that anything that can be written as a gauged linear σ -model evades instanton effects.

It was recently observed in [10, 11] that resolutions of orbifolds can see instanton effects. Here we really can compare conformal field theory and geometry to get nontrivial statements. It was shown in [11] that while the count of deformations of the conformal field theory makes no reference to a choice of resolution, the number of deformations of the tangent sheaf does depend on this choice. This difference must be due to instantons.

Interestingly, one favoured choice of resolution, the Hilbert scheme, always agrees with conformal field theory [12]. Instantons are therefore associated with deviations of a resolution from the Hilbert scheme. We will use this approach to systematically look for instanton effects below.

In section 2 we will review how to count the number of (0,2)-deformations in an orbifold conformal field theory and how to count deformations of the tangent bundle of a noncompact toric Calabi–Yau threefold. Simple diagrammatical methods using quivers from the toric data from [11] make the analysis straight-forward even though we need to use fairly large groups for G .

In section 3 we review the necessary material for worldsheet instantons and how splitting types of bundles is central. In section 4 we analyze the geometry of splitting and see exactly how to hunt for instantons in the case the rational curves are smooth and toric. While we find some instantons, we do not find enough and in section 5 we briefly discuss other possible sources such as reducible curves and multiple covers. We should emphasize that since we are doing (0,2)-deformations, we do *not* simply reproduce Gromov–Witten theory in such cases.

2 Counting Deformations

In this section we review the results of [11] where we see the discrepancy between the orbifold conformal field theory computation and the geometric computation of the number of deformations of the tangent bundle.

Let $G \subset \text{SL}(3)$ be a finite Abelian group. We are then considering the orbifold \mathbb{C}^3/G and we will assume that G has an *isolated* fixed point at the origin. We denote the resolution of \mathbb{C}^3/G by X or X_Σ .

2.1 Orbifold Conformal Field Theory

Let $g \in G$ and diagonalize the action on \mathbb{C}^3 as

$$(z_1, z_2, z_3) \mapsto (e^{2\pi i\nu_1} z_1, e^{2\pi i\nu_2} z_2, e^{2\pi i\nu_3} z_3), \quad (2)$$

where $0 \leq \nu_i < 1$. Define $\tilde{\nu}_i = \nu_i - \frac{1}{2} - m$, where $m \in \mathbb{Z}$ such that $-1 < \tilde{\nu}_i \leq 0$.

We may enumerate the number of massless fields corresponding to deformations as follows paraphrasing [11,13]. We get contributions from each g -twisted sector when g satisfies

$$\sum_i \nu_i = 1. \quad (3)$$

Note that in this case, at most one of the ν_i 's can be greater than $\frac{1}{2}$. For each g -twisted sector satisfying (3) the contribution is given by the coefficient of $q^0 z^0$ in the power series expansion of the partition function

$$Z = q^a z^b \prod_{i=1}^3 \frac{(1 + z^{-1} q^{1+\tilde{\nu}_i}) (1 + z q^{-\tilde{\nu}_i})}{(1 - q^{\nu_i}) (1 - q^{1-\nu_i})}, \quad (4)$$

where

$$(a, b) = \begin{cases} (-\frac{1}{2}, -1) & \text{if all } \nu_i \leq \frac{1}{2} \\ (-\nu_i, 0) & \text{if } \nu_i > \frac{1}{2} \end{cases} \quad (5)$$

Adding the contributions of all such g 's together we get the total number of first order deformations. Some of these are deformations preserving the (2,2) supersymmetry (counted by the number of g 's satisfying (3)) and correspond to blow-up Kähler deformations. The remainder should be deformations of the tangent bundle.

A key point to emphasize here is that the conformal field theory count makes no reference to a resolution of the singularity and thus, obviously, cannot depend on the choice of resolution.

It should be noted that the number of (0,2)-deformations is not an invariant over the moduli space and can increase on lower-dimensional strata [14]. This can most easily be seen in Landau–Ginzburg models and was analyzed in detail in [13]. This effect does not seem to be present in resolutions of \mathbb{C}^3/G . The Hilbert scheme count agrees perfectly with the conformal field theory count [12]. It is possible that the orbifold conformal field theory count has “extra” moduli which disappear when the blow-up is turned on. Then the Hilbert scheme would need to have instanton corrections to lower its count by the same margin. This coincidence seems very unlikely and we prove that there are no instantons in the form of toric curves later in this paper. We will therefore ignore this possibility. It certainly does not help resolve the issue of lack of instantons in this paper — it would make it worse.

2.2 Geometry

Now we review how to compute the number of deformations of the tangent bundle of a toric variety. To fix notation, we need to quickly review the basic construction of toric geometry. We refer to [15] for all the details. Begin with

$$0 \longrightarrow \mathbb{M} \xrightarrow{\mathcal{A}} \mathbb{Z}^{\oplus n} \xrightarrow{\Phi} \mathbb{D} \longrightarrow 0, \quad (6)$$

where \mathbf{M} is a lattice of rank d . \mathcal{A} is an $n \times d$ matrix. The rows of \mathcal{A} give the coordinates of a set of n points in the lattice \mathbf{N} dual to \mathbf{M} . We will use the same symbol \mathcal{A} to denote this point set. Each point is associated to a homogeneous coordinate x_i , $i = 1, \dots, n$. We then have a homogeneous coordinate ring $S = \mathbb{C}[x_1, \dots, x_n]$.

\mathbf{D} is an abelian group which induces an action on the homogeneous coordinates as follows. Let $r = n - d$ denote the rank of \mathbf{D} . Then $\mathbf{D} \otimes_{\mathbb{Z}} \mathbb{C}^* = (\mathbb{C}^*)^r$ acts on the homogeneous coordinates with charges given by the matrix Φ . If \mathbf{D} has a torsion part H , then, in addition to $(\mathbb{C}^*)^r$, we have a finite group action of H on the homogeneous coordinates the charges of which are given by the kernel of the matrix \mathcal{A}^t acting on $(\mathbb{Q}/\mathbb{Z})^{\oplus n}$.

The fan Σ is defined as a fan over a simplicial complex with vertices \mathcal{A} . This combinatorial information defines an ideal $B \subset S$ as explained in [15]. The toric variety X_{Σ} is then given by the quotient

$$X_{\Sigma} = \frac{\text{Spec } S - V(B)}{(\mathbb{C}^*)^r \times H}. \quad (7)$$

The homogeneous coordinate ring $S = \mathbb{C}[x_1, \dots, x_n]$ is multigraded by the free module \mathbf{D} :

$$S = \bigoplus_{\mathbf{d} \in \mathbf{D}} S_{\mathbf{d}}. \quad (8)$$

Let $S(\mathbf{q})$ be the free S -module with grades shifted so that $S(\mathbf{q})_{\mathbf{d}} = S_{\mathbf{q}+\mathbf{d}}$ as usual. Line bundles or invertible sheaves $\mathcal{O}(\mathbf{q})$ on X_{Σ} are then associated to modules $S(\mathbf{q})$ for any $\mathbf{q} \in \mathbf{D}$.

In the case X is a Calabi–Yau variety, all the points \mathcal{A} lie in a hyperplane in \mathbf{N} . The orbifold singularity \mathbb{C}^3/G can always be completely resolved crepantly by taking \mathcal{A} to contain all the points of \mathbf{N} in its interior hull and taking Σ to be a fan over a simplicial complex including all the new points of \mathcal{A} . Let Δ denote this simplicial complex. Each triangle in Δ has area $\frac{1}{2}$, \mathbf{D} is torsion-free and X_{Σ} is smooth. Note that the condition that G has an isolated fixed point means that points in \mathcal{A} are either vertices of the triangle Δ or properly in the interior.

The supersymmetric conformal field theory requires a Kähler form on X and so we insist X is projective. This requires the triangulation of Δ to be “regular” or “coherent” in the sense of [16].

A *toric rational curve* is a rational curve in X_{Σ} which is invariant under the $(\mathbb{C}^*)^d$ torus action. Because of the “orbit-cone correspondence”, such rational curves correspond to edges of the graph giving the triangulation of Δ . For the curve to be compact, the edge must be in the interior of Δ . Thus, the edge is the edge of two triangles. By a choice of coordinates on Δ , we may always make the edge look like figure 1 for some $m \in \mathbb{Z}$. Points $i, j, \alpha, \beta \in \mathcal{A}$ correspond to divisors which we denote D_i etc. The rational curve is $C = D_i \cap D_j$. This curve intersects each of the divisors D_{α} and D_{β} transversely at a point. We will review in section 4.2 that the normal bundle of this curve is then

$$\mathcal{N} = \mathcal{O}(-1 - m) \oplus \mathcal{O}(-1 + m), \quad (9)$$

and we refer to it as a $(-1 - m, -1 + m)$ -curve. For each curve $C_{ij} = D_i \cap D_j$ we may assume $m_{ij} \geq 0$ by reversing i and j in figure 1 as necessary. If $m > 0$ this fixes the direction of the

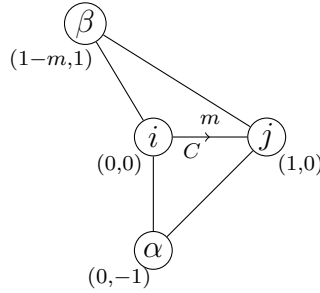


Figure 1: A toric curve $C = D_i \cap D_j$.

arrow in the figure — it always points “away” from β . These arrows will be important when analyzing instanton corrections later in the paper. When $m = 0$ there will be no arrow and we will draw a dotted line between i and j . Note that the coordinates x_α and x_β associated with the corresponding points in figure 1 can be used as the homogeneous coordinates on C_{ij} .

We will explore how to count deformations of the tangent bundle in section 4.1 but, for now, we will just quote the result from [11]. The number of blow-up modes plus framed deformations of the tangent bundle is given by

$$3n_{\text{int}} + \sum_{C_{ij}} m_{ij}, \quad (10)$$

where n_{int} is the number of internal points in Δ . Each toric curve C_{ij} is counted once in (10) where we order i and j so that $m_{ij} \geq 0$.

2.3 A \mathbb{Z}_{11} Example

To illustrate the above computations consider \mathbb{C}^3/G where $G \cong \mathbb{Z}_{11}$ generated by g with $(\nu_1, \nu_2, \nu_3) = (\frac{1}{11}, \frac{2}{11}, \frac{8}{11})$. The elements of G satisfying (3) are then g, g^2, g^3, g^6, g^7 which yield 14,4,5,7,9 moduli respectively. Thus the exact conformal field theory computation dictates that there must be 39 (0,2) deformations (of which 5 are associated to blow-up modes giving (2,2) deformations).

Now consider the geometric computation. There are 5 different possible crepant resolutions of this orbifold all of which are projective. These, and the associated values of m_{ij} are shown in figure 2.¹ The interior dotted lines represent $m_{ij} = 0$, i.e., $(-1, -1)$ -curves. The border of the triangle is shown as dotted as that also makes no contribution to the count. The number appearing in a box to the left of each resolution is the total count (10).

So, the first two resolutions in figure 2 are in agreement with conformal field theory while the other three have an excess in the geometric count. This difference must be due to worldsheet instanton effects.

¹This figure also appeared in [11] but the numbers have changed slightly due to a change in some definitions.

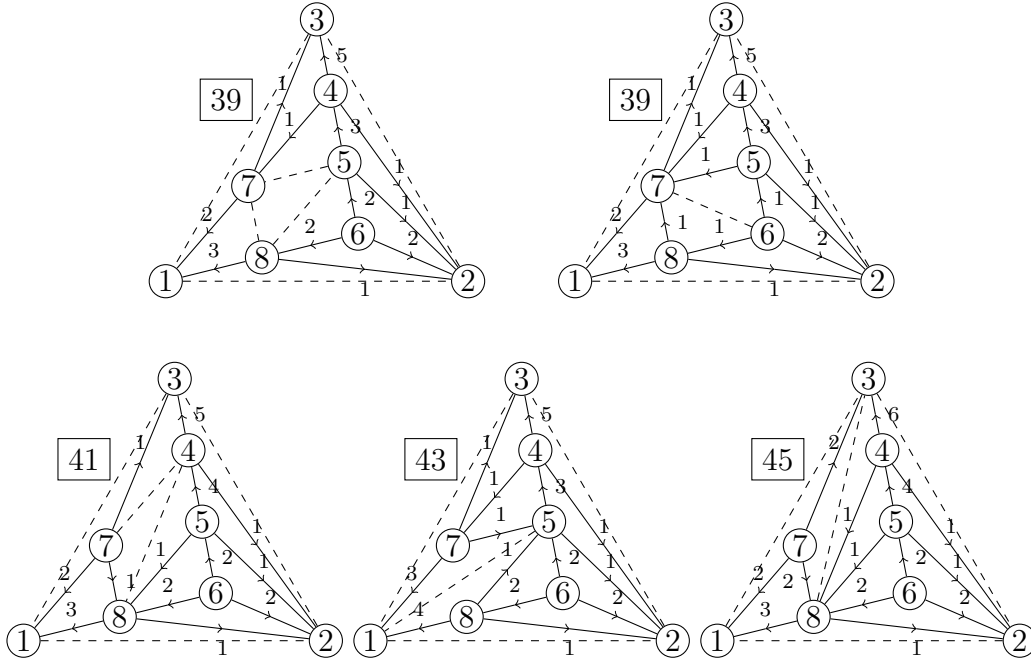


Figure 2: The five resolutions of $\mathbb{C}^3/\mathbb{Z}_{11}$.

Note that the first of the resolutions in figure 2 is the distinguished resolution of the Hilbert scheme. This always has a minimal number of $(0,2)$ -deformations and does not require any instanton corrections to agree with conformal field theory [12]. We will prove that no toric irreducible rational curves give instanton corrections to the Hilbert scheme in section 5.1. So conformal field theory and geometry agree nicely in this case.

2.4 Deviations from the Hilbert Scheme

To get a better idea of the Hilbert scheme we show the case $G \cong \mathbb{Z}_{53}$, with $(\nu_1, \nu_2, \nu_3) = (\frac{1}{53}, \frac{7}{53}, \frac{45}{53})$, in figure 3. We do not show the values of m to avoid cluttering the diagram. The general following structure was proved in [17]:²

Proposition 1 *If we draw a triangulation Δ corresponding to the Hilbert scheme of \mathbb{C}^3/G using arrows and dotted lines as in section 2.2 then*

1. *There is a set of “big” triangles (of possibly non-minimal area) with non-dotted edges. These triangles are “equilateral” with respect to counting lattice points in the edges. The arrows on the edges of these triangles all point towards an outer vertex where the line terminates.*

²The arrows as defined in [17] point in the opposite directions to ours. We choose our orientation to coincide with the directions of associated Ext groups.

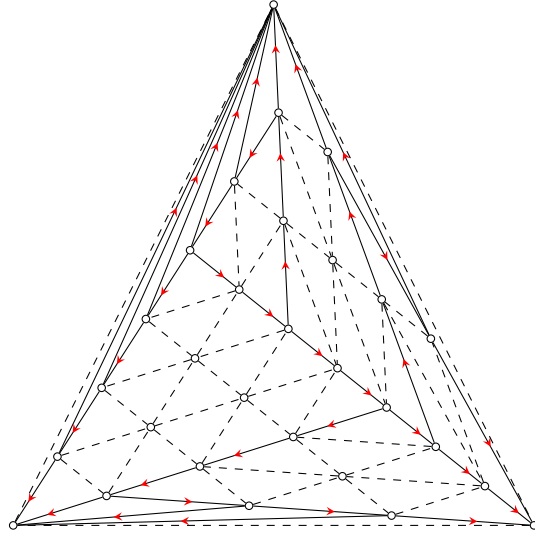


Figure 3: Hilbert Scheme Resolution for $G = \mathbb{Z}_{53}$.

2. Each of the above big equilateral triangles is subdivided, if necessary, with dotted lines into a set of similar triangles of minimal area.

A nice systematic way to hunt for instanton effects is to deviate from the Hilbert scheme. Consider $\mathbb{C}^3/\mathbb{Z}_n$ for a very large value of n . The sizes of the “big” triangles depend on the choice of weights but there will be a choice of weights for which at least one of these triangles is very big. Then Δ for this Hilbert scheme will contain a regular tessellation with a large number of small triangles. Within this regular tessellation the toric rational curves are all of type $(-1, -1)$. Now perturb this regular tessellation by performing a flop. Any non- $(-1, -1)$ -curves produced will add extra $(0,2)$ -deformations and thus must be associated to instanton effects.

This simplest such modification to form a lattice “defect” is shown in figure 4. Relative to the Hilbert scheme, it adds 4 to the geometric count of deformations of \mathcal{T} . Since this should have the same number of $(0,2)$ -deformations as the Hilbert scheme, all 4 of the deformations of \mathcal{T} must be obstructed by instantons. We analyze this in section 4.4.1.

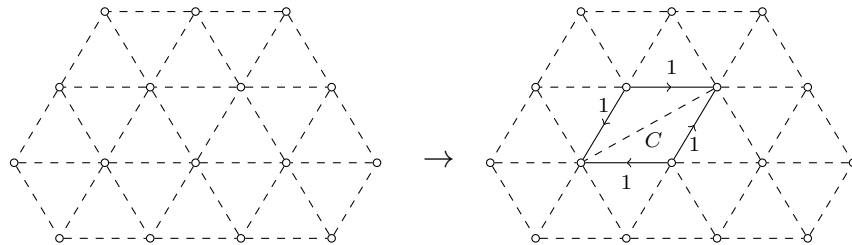


Figure 4: A simple lattice defect

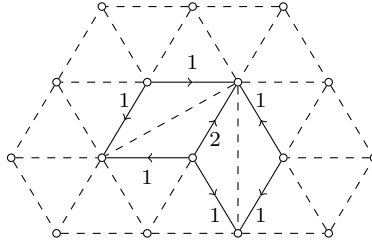


Figure 5: Complimentary Lattice Defects

So if we have a single flop on the interior of a regular triangular lattice, it induces 4 deformations that correspond to the instanton corrections. What happens as we introduce more flops?

Proposition 2 *If we take n flops of a regular lattice structure, it adds between $4\sqrt{n}$ and $4n$ deformations of \mathcal{T}*

We first show that the most deformations that correspond to n flops is $4n$. Anytime we take a flop, it adds at most 4 deformations (one for each curve that shares a triangle with the changed curve). Thus, if each of n flops adds 4 deformations, we have $4n$ deformations. There are two ways this can occur. If all of the flops are isolated, we end up with n parallelograms that look like figure 4, where each arrow has multiplicity 1. It is also possible that any number of the defects be adjacent, but changed in a complimentary way. An example where this occurs can be seen in figure 5. In this case every arrow has multiplicity 1 or 2, and the total number of deformations is still $4n$.

We now show that the lower bound on the number of deformations is given by $4\sqrt{n}$. This bound is achieved when \sqrt{n} is an integer, and all of the flops occur within a \sqrt{n} by \sqrt{n} quadrilateral. Each time we take a flop, we want to minimize the number of deformations added. This means we must have as many $(-1, -1)$ -curves as possible. This is done by taking flops that border the deformations we already have (which correspond to $(-2, 0)$ -curves), so that they become $(-1, -1)$ -curves again. If one such curve is changed in this way, then this flop adds two deformations (instead of the 4 we saw earlier). If two are changed, then this flop does not change the number of deformations. Each time a flop is added, use the one that changes as many curves in this way as is possible. If we follow this algorithm, beginning with a single defect as in figure 4, we spiral outward. It is clear that this minimizes the total number of deformations. We also see that whenever these flops occur in a $\sqrt{n} \times \sqrt{n}$ quadrilateral, there are a total of $4\sqrt{n}$ deformations. Since this process adds 2 deformations with the next flop, and another 2 deformations halfway to the next perfect quadrilateral, the total number of deformations is always at least $4\sqrt{n}$. \square

Figure 6 shows an example which achieves this lower bound, in the case where there are 4 total flops. We note that there are no “interior” deformations. This is always the case when following the above minimization procedure. We also note that all arrows have multiplicity 1.

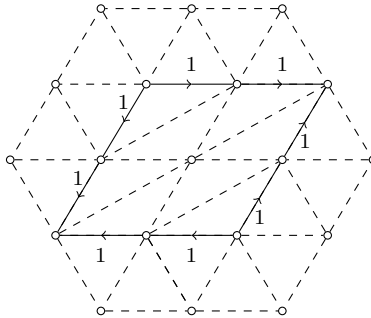


Figure 6: Minimizing Lattice Defects

Lattice defects within the regular tessellation always lead to an even number of deformations, and every even integer between $4\sqrt{n}$ and $4n$ can be achieved as the number of deformations by using a combination of the above methods. It is also possible to obtain arrows with multiplicities higher than two, through a combination of the methods described above.

3 Worldsheet Instantons

For the supersymmetric non-linear σ -model with target space X , the instantons are given by holomorphic maps from the string worldsheet to X [2]. In an instanton calculation the path integral is reduced to an integral over the moduli space of the instanton solutions. In the presence of fermions this will usually be a supermoduli space. Thus, when computing an instanton correction to a correlation functions, we get a zero value if the number of fermions in the integrand is not equal to the number of fermions in the supermoduli space measure.

An alternative approach to computing instantons is to view one intrinsically as a subspace of X and use the physics of D-branes [18]. When the contribution is nonzero, this gives a slightly more practical methods for computing corrections to the superpotential as done in [19], for example. The disadvantage is that this requires the assumption that the instanton image is a smooth curve. We will therefore use the older method coming from conformal field theory.

Let ϕ be the σ -model map from the worldsheet to X . We then have left-moving fermions taking values in $K^{\frac{1}{2}} \otimes \phi^*(V \oplus \bar{V})$, where K is the canonical bundle of the worldsheet, i.e., $K \cong \mathcal{O}(-2)$. Left-moving fermion zero modes are holomorphic sections of this bundle:

$$\begin{aligned} H^0(K^{\frac{1}{2}} \otimes \phi^*(V)) &= H^0(\phi^*(V) \otimes \mathcal{O}(-1)) \\ H^0(K^{\frac{1}{2}} \otimes \phi^*(\bar{V})) &= H^1(\phi^*(V) \otimes \mathcal{O}(-1)), \end{aligned} \tag{11}$$

where the second line follows from Serre duality and $\bar{V} \cong V^\vee$. The right-moving fermions take values in $\bar{K}^{\frac{1}{2}} \otimes (\mathcal{T} \oplus \bar{\mathcal{T}})$. The zero modes are antiholomorphic sections of this bundle. The easiest thing to do is to take the complex conjugate and look at holomorphic sections

again. Thus the zero modes are

$$\begin{aligned} H^0(K^{\frac{1}{2}} \otimes \phi^*(\mathcal{I})) &= H^0(\phi^*(\mathcal{I}) \otimes \mathcal{O}(-1)) \\ H^0(K^{\frac{1}{2}} \otimes \phi^*(\overline{\mathcal{I}})) &= H^1(\phi^*(\mathcal{I}) \otimes \mathcal{O}(-1)). \end{aligned} \tag{12}$$

For this section we suppose the instanton is an *embedding* of the worldsheet with image a rational curve $C \subset X$. Then we may identify $\phi^*(V)$ with the restriction $V|_C$. All vector bundles over a rational curve split into a sum of line bundles and V is rank three. Thus

$$V|_C = \mathcal{O}(a) \oplus \mathcal{O}(b) \oplus \mathcal{O}(c), \tag{13}$$

where $a + b + c = c_1(V) = 0$. The number of left-moving fermion zero modes, from (11), is $|a| + |b| + |c|$.

Now let us consider the right-moving fermions zero modes by replacing V with \mathcal{I} . The adjunction formula tells us there is an exact sequence

$$0 \longrightarrow \mathcal{I}_C \longrightarrow \mathcal{I}|_C \longrightarrow \mathcal{N} \longrightarrow 0, \tag{14}$$

where $\mathcal{I}_C \cong \mathcal{O}(2)$. This exact sequence need not split. Indeed we will see an example in section 5.4 where $\mathcal{I}|_C$ does not include a $\mathcal{O}(2)$ factor. Having said that, we will show in section 4.2 that (14) always splits when C is toric.

Since $\mathcal{N} \cong \mathcal{O}(k) \oplus \mathcal{O}(l)$ we see C is a (k, l) -curve. Clearly $k + l = -2$. If neither k nor l is greater than 3 then $\text{Ext}^1(\mathcal{N}, \mathcal{I}_C) = 0$ and so (14) splits again. A first-order deformation of $C \subset X$ corresponds to a section of \mathcal{N} . Thus, the case $k = l = -1$ has no deformations and the $(-1, -1)$ -curve C is isolated. The converse is not, in general, true. Any curve other than $(-1, -1)$ will have first order deformations but these deformations may be obstructed and thus the curve may still be isolated. See [20] for a detailed example. Luckily, toric varieties do not suffer from such obstructions. That is because the normal bundle of C is explicitly a Zariski open set in X . Thus, in this paper, rational curves are isolated if and only if they are $(-1, -1)$ -curves.

The case considered in [3] was for a $(-1, -1)$ -curve. The right-moving sector, where the fermions take values in $\mathcal{I}|_C = \mathcal{O}(2) \oplus \mathcal{O}(-1) \oplus (-1)$ therefore has 4 zero modes. If V is suitably generic then $a = b = c = 0$ and thus there are no left-moving zero modes. It is precisely this case where the fermionic dimensions work out to give a potentially nonzero instanton correction to the superpotential. These theories are therefore “bad”. A first order deformation of the tangent bundle to such a V should not correspond to a massless state.

In this paper we are concerned only with the question of whether instanton corrections are nonzero or not. To actually compute the magnitude it is necessary to compute Pfaffians and determinants. See [19] for an example. Here we note that, at least in the case of a smooth $(-1, -1)$ -curve, the contribution is nonzero if and only if the fermion zero mode count is as above.

If C is not a $(-1, -1)$ -curve it will move in a family. This may, or may not lead to extra right-moving fermion zero modes. If it does, this will change the condition for instanton corrections for V to something other than the trivial splitting $a = b = c = 0$. We will discuss this in section 5.1.

4 Splitting

4.1 Deformations of \mathcal{T} .

Let \mathbf{q}_i denote the multi-degree, or “charge”, of x_i . It was shown in [21] that the tangent sheaf \mathcal{T} of X_Σ is given by

$$0 \longrightarrow \mathcal{O}^{\oplus r} \xrightarrow{E} \bigoplus_{i=1}^n \mathcal{O}(\mathbf{q}_i) \longrightarrow \mathcal{T} \longrightarrow 0, \quad (15)$$

where E is an $n \times r$ matrix whose (i, j) -th entry is $\Phi_{ji}x_i$ and Φ is the matrix in (6). It is important to note that each summand in middle term of (15) corresponds to a point in \mathcal{A} and thus a point in our toric diagrams. This is central to way we will visualize the constructions below.

It follows from (15) that $\mathcal{H}om(\mathcal{T}, \mathcal{T})$ is isomorphic in $\mathbf{D}(X)$ to the complex

$$0 \longrightarrow \bigoplus_i \mathcal{O}(-\mathbf{q}_i)^{\oplus r} \longrightarrow \begin{array}{c} \mathcal{O}^{\oplus r^2} \\ \oplus \\ \bigoplus_{i,j} \mathcal{O}(\mathbf{q}_i - \mathbf{q}_j) \end{array} \longrightarrow \bigoplus_i \mathcal{O}(\mathbf{q}_i)^{\oplus r} \longrightarrow 0. \quad (16)$$

We can then use the hypercohomology spectral sequence to compute the space of first order deformations of \mathcal{T} which is $\text{Ext}^1(\mathcal{T}, \mathcal{T}) = H^1(X, \mathcal{H}om(\mathcal{T}, \mathcal{T}))$. We are doing a simpler version of the computation that appeared in [10, 13].

Note that many of the cohomology groups vanish:

Proposition 3 *Let α be a vertex of Δ and let D_α be the associated toric divisor. Then*

$$\begin{aligned} H^i(\mathcal{O}_{D_\alpha}(\mathbf{q}_\alpha)) &= 0, & \text{for } i = 0, 1, \alpha \text{ interior} \\ H^1(\mathcal{O}(\mathbf{q}_\alpha)) &= 0, \\ H^i(\mathcal{O}(-\mathbf{q}_\alpha)) &= 0, & \text{for } i = 1, 2. \end{aligned} \quad (17)$$

To prove the first line note that $\mathcal{O}_{D_\alpha}(-\mathbf{q}_\alpha)$ is the conormal bundle of D_α . Thus, since X is Calabi–Yau, by adjunction we have that $\mathcal{O}_{D_\alpha}(\mathbf{q}_\alpha)$ is the canonical bundle of D_α . The fact that α is an interior point means that D_α is compact. Now use Serre duality and the fact that $H^i(\mathcal{O}_{D_\alpha}) = 0$ for $i > 0$, since D_α is a rational surface. If α is interior then other two results follow from the first result and the short exact sequences

$$0 \longrightarrow \mathcal{O}(\mathbf{a}) \longrightarrow \mathcal{O}(\mathbf{a} + \mathbf{q}_\alpha) \longrightarrow \mathcal{O}_{D_\alpha}(\mathbf{q}_\alpha) \longrightarrow 0, \quad (18)$$

for $\mathbf{a} = 0$ and $-\mathbf{q}_\alpha$ respectively. If α is a vertex of the triangle then $\mathcal{O}(\mathbf{q}_\alpha)$ is a “tautological line bundle” in the McKay correspondence as in [22]. These, and \mathcal{O} , are projective objects in the category of coherent sheaves and thus the required cohomology groups vanish. ■

The spectral sequence is therefore quite easy to compute and the result is that we have two contributions to $\text{Ext}^1(\mathcal{T}, \mathcal{T})$ with obvious interpretations:

1. $\bigoplus_i H^0(\bigoplus_i \mathcal{O}(\mathbf{q}_i)^{\oplus r})$ contributes deformations of the map E in (15).³
2. $\bigoplus_{i,j} H^1(\mathcal{O}(\mathbf{q}_i - \mathbf{q}_j))$ gives deformations of the direct sum in the middle of (15).

The first type of deformations, the deformations of E , should be viewed as the “easy” deformations. They have been much-studied in the context of the gauged linear σ -model [9, 23, 24]. These do not depend on the choice of resolution and we will see in section 4.3 that they never suffer from instanton corrections. The second type of deformations are the focus of this paper.

4.2 Restricting the Tangent Bundle

Let us restrict the presentation of \mathcal{T} from (15) to the $(-1 - m, -1 + m)$ curve C appearing in figure 1. This curve is given by $x_i = x_j = 0$ with homogeneous coordinate $[x_\alpha, x_\beta]$. Let ζ_k denote one of the $n - 4 = r - 1$ elements of \mathcal{A} not appearing in figure 1 and let x_{ζ_k} be the associated coordinate. There is only one \mathbb{C}^* -action in $(\mathbb{C}^*)^r$ that leaves all the x_{ζ_k} ’s invariant. This comes from the affine relation between the 4 points in figure 1 and yields a charge Q given by:

$$Q \left| \begin{array}{cccc} x_\alpha & x_\beta & x_i & x_j \\ \hline 1 & 1 & -1 - m & -1 + m \end{array} \right. \quad (19)$$

It follows that tangent sheaf restricts to C as the cokernel of the map

$$\mathcal{O}^{\oplus r} \xrightarrow{E} \mathcal{O}(1)^{\oplus 2} \oplus \mathcal{O}(-1 - m) \oplus \mathcal{O}(-1 + m) \oplus \mathcal{O}^{\oplus r-1}, \quad (20)$$

where \mathcal{O} is now, of course, the structure sheaf of C . Now, since $\{i, j, \zeta_k\}$ do not form the vertices of a simplex in the triangulation of Δ , $(x_i, x_j, x_{\zeta_k}) \supset B$. Thus, on C where $x_i = x_j = 0$ we must have $x_{\zeta_k} \neq 0$. This gives a great deal of redundancy in the presentation (20). We may cancel $r - 1$ of the \mathcal{O} ’s to give

$$0 \longrightarrow \mathcal{O} \xrightarrow{\begin{pmatrix} x_\alpha \\ x_\beta \\ 0 \\ 0 \end{pmatrix}} \mathcal{O}(1)^{\oplus 2} \oplus \mathcal{O}(-1 - m) \longrightarrow \mathcal{T}|_C \longrightarrow 0. \quad (21)$$

$$\oplus \mathcal{O}(-1 + m)$$

But there is a short exact sequence on C :

$$0 \longrightarrow \mathcal{O} \xrightarrow{\begin{pmatrix} x_\alpha \\ x_\beta \end{pmatrix}} \mathcal{O}(1)^{\oplus 2} \xrightarrow{\begin{pmatrix} -x_\beta & x_\alpha \end{pmatrix}} \mathcal{O}(2) \longrightarrow 0, \quad (22)$$

from which it follows that

$$\mathcal{T}|_C = \mathcal{O}(2) \oplus \mathcal{O}(-1 - m) \oplus \mathcal{O}(-1 + m), \quad (23)$$

as promised.

³Some of these are killed by the d_1 differential in the spectral sequence. This amounts to subtracting simple reparametrizations from the count as explained in [13]. Care must be taken in this step to count *framed* deformations. This is done in [11].

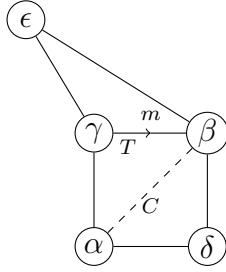


Figure 7: Part of Δ used in restricting deformations.

4.3 Restricting the Deformation

In this section we will restrict a deformation of the tangent bundle to a toric rational curve $C \subset X$. First we prove the following, which will be enough to prove that worldsheet instantons never obstruct the “easy” deformations of \mathcal{T} .

Proposition 4 *First order deformations of \mathcal{T} coming from first order deformations of the map E in (15) will always give $\mathcal{O}(-1 - m)$ as a summand when restricted to C .*

To see this note that the fact we consider only small deformations means that we assume the nonzero entries in E coming from the condition $x_{\zeta_k} \neq 0$ remain nonzero and we may still cancel the $r - 1$ \mathcal{O} ’s to get (21). Furthermore, since x_α and x_β have positive degree, we cannot have any nonzero expression in the third entry of the matrix appearing over the first map in (21). Therefore, the $\mathcal{O}(-1 - m)$ summand must be preserved unchanged in the cokernel of this map. ■

So now we turn to the “hard” deformations associated to $H^1(\mathcal{O}(\mathbf{q}_\beta - \mathbf{q}_\gamma))$. We can study these very explicitly using the local cohomology picture of sheaf cohomology in toric varieties from [25].

For the sake of exposition we will assume that C is a $(-1, -1)$ -curve. Then let us restrict attention to an internal part of the triangulation of Δ that looks like figure 7. Let $x_\alpha, \dots, x_\epsilon$ be the corresponding homogeneous variables. C is then the $(-1, -1)$ -curve given by $x_\alpha = x_\beta = 0$ and let T be the $(-1 - m, -1 + m)$ -curve given by $x_\beta = x_\gamma = 0$. We are going to be interested in worldsheet instantons over C associated to hard $H^1(\mathcal{O}(\mathbf{q}_\beta - \mathbf{q}_\gamma))$ deformations originating from T . We will first confirm the result stated earlier that this contributes m first order deformations of the tangent bundle.

From the sequence,

$$0 \longrightarrow \mathcal{O}(-\mathbf{q}_\gamma) \xrightarrow{x_\beta} \mathcal{O}(\mathbf{q}_\beta - \mathbf{q}_\gamma) \longrightarrow \mathcal{O}_{D_\beta}(\mathbf{q}_\beta - \mathbf{q}_\gamma) \longrightarrow 0, \quad (24)$$

it follows from proposition 3 that

$$H^1(\mathcal{O}(\mathbf{q}_\beta - \mathbf{q}_\gamma)) \cong H^1(\mathcal{O}_{D_\beta}(\mathbf{q}_\beta - \mathbf{q}_\gamma)). \quad (25)$$

Furthermore, using

$$0 \longrightarrow \mathcal{O}_{D_\beta}(\mathbf{q}_\beta - \mathbf{q}_\gamma) \xrightarrow{x_\gamma} \mathcal{O}_{D_\beta}(\mathbf{q}_\beta) \longrightarrow \mathcal{O}_T(\mathbf{q}_\beta) \longrightarrow 0 \quad (26)$$

and proposition 3 we see that $H^1(\mathcal{O}_{D_\beta}(\mathbf{q}_\beta - \mathbf{q}_\gamma)) \cong H^0(\mathcal{O}_T(\mathbf{q}_\beta))$. Thus we may explicitly count the desired deformations by analyzing holomorphic functions on T with the correct charge. As in section 4.2, let ζ_k denote a vertex in Δ that does not appear in figure 7. So $x_{\zeta_k} \neq 0$ on T and we may use the $(\mathbb{C}^*)^r$ -action to fix $x_{\zeta_k} = 1$. That is, we only consider functions of $x_\alpha, \dots, x_\epsilon$. Two of the $(\mathbb{C}^*)^r$ actions have charges

$$\begin{array}{c|ccccc} & x_\alpha & x_\beta & x_\gamma & x_\delta & x_\epsilon \\ \hline Q_1 & -1 & -1 & 1 & 1 & 0 \\ Q_2 & 1 & -1 - m & -1 + m & 0 & 1 \end{array} \quad (27)$$

with charge zero for every vertex not appearing in figure 7.

These charges can be used to determine a basis of monomials for $H^0(\mathcal{O}_T(\mathbf{q}_\beta))$, i.e., holomorphic functions on T with the same charge as x_β . Obviously we can't use x_β and x_γ since they are zero on T . The coordinates x_α and x_ϵ have zeros on T but x_δ does not. Thus, we can have non-negative powers of x_α and x_ϵ , and any power of x_δ . A basis is thus given by the m monomials

$$x_\alpha^{m-1} x_\delta^{m-2}, x_\alpha^{m-2} x_\epsilon x_\delta^{m-3}, x_\alpha^{m-3} x_\epsilon^2 x_\delta^{m-4}, \dots, x_\alpha x_\epsilon^{m-2}, x_\epsilon^{m-1} x_\delta^{-1}. \quad (28)$$

So, as promised, we contribute m first order deformations of the tangent bundle. Furthermore, we have an explicit realization of these deformations which allows us to restrict to C .

First map the holomorphic functions in $H^0(\mathcal{O}_T(\mathbf{q}_\beta))$ to rational functions representing local cohomology associated to $H^1(\mathcal{O}_{D_\beta}(\mathbf{q}_\beta - \mathbf{q}_\gamma))$ using the connecting homomorphism in the long exact sequence associated to (26). This is clearly given by division by x_γ . Then we restrict to C by setting $x_\alpha = x_\beta = 0$. Finally we may set $x_\epsilon = 1$ by using a \mathbb{C}^* -action since $x_\epsilon \neq 0$ on C . Thus the restriction map sends all the monomials in (28) to zero except the final one which becomes

$$\frac{1}{x_\gamma x_\delta}. \quad (29)$$

This is precisely the monomial which in local cohomology represents $H^1(C, \mathcal{O}(-2)) \cong \mathbb{C}$. Therefore, restriction gives us a surjective map

$$\rho_C : H^1(\mathcal{O}_{D_\beta}(\mathbf{q}_\beta - \mathbf{q}_\gamma)) \rightarrow H^1(C, \mathcal{O}(-2)). \quad (30)$$

This deformation comes from $\text{Ext}_X^1(\mathcal{O}(\mathbf{q}_\gamma), \mathcal{O}(\mathbf{q}_\beta))$ which restricts to $\text{Ext}_C^1(\mathcal{O}(1), \mathcal{O}(-1))$. The nontrivial extension of $\mathcal{O}(1)$ by $\mathcal{O}(-1)$ on \mathbb{P}^1 is $\mathcal{O} \oplus \mathcal{O}$ (see appendix). This is how we deform $\mathcal{S}|_C$ in (20).

4.4 Examples

4.4.1 The simple defect case

Let us apply the above result to the simple lattice defect in figure 4. Here we have a $(-1, -1)$ -curve labeled C which intersects four $(-2, 0)$ -curves. The worldsheet instanton will be associated to C and the extra deformations of \mathcal{T} , which we need to kill, are associated to these four $(-2, 0)$ -curves. Let $[x, y]$ be the homogeneous coordinates on C .

This is the case $m = 1$ of the previous section. Each arrow in figure 4 is associated to $\text{Ext}_C^1(\mathcal{O}(1), \mathcal{O}(-1)) \cong \mathbb{C}$. In terms of $\mathcal{T}|_C$, these can be viewed as the four dotted lines in:

$$\begin{array}{c}
 \mathcal{O}(1) \\
 \oplus \\
 \mathcal{O}(1) \\
 \oplus \\
 \mathcal{O}(-1) \\
 \oplus \\
 \mathcal{O}(-1)
 \end{array}
 \xrightarrow{\begin{pmatrix} x & 0 \\ y & 0 \\ 0 & 0 \end{pmatrix}}
 \mathcal{T}|_C \longrightarrow 0, \tag{31}$$

$0 \longrightarrow \mathcal{O} \longrightarrow \begin{array}{c} \mathcal{O}(1) \\ \oplus \\ \mathcal{O}(1) \\ \oplus \\ \mathcal{O}(-1) \\ \oplus \\ \mathcal{O}(-1) \end{array} \longrightarrow \mathcal{T}|_C \longrightarrow 0,$

where each dotted line wants to turn $\mathcal{O}(1) \oplus \mathcal{O}(-1)$ into $\mathcal{O} \oplus \mathcal{O}$.

To analyze this more carefully we will rewrite this presentation of $\mathcal{T}|_C$ such that these deformations can be written simply as deformations of maps in the complex. Replace each $\mathcal{O}(1)$ by the quasi-isomorphic $\mathcal{O}(-1) \rightarrow \mathcal{O}^{\oplus 2}$ (as in the appendix) and reduce the presentation to get

$$0 \longrightarrow \mathcal{O}(-1)^{\oplus 2} \xrightarrow{\begin{pmatrix} x & 0 \\ y & x \\ 0 & y \\ a & b \\ c & d \end{pmatrix}} \begin{array}{c} \mathcal{O}^{\oplus 3} \\ \oplus \\ \mathcal{O}(-1)^{\oplus 2} \end{array} \longrightarrow \mathcal{T}|_C \longrightarrow 0, \tag{32}$$

where $a = b = c = d = 0$. Now we see the 4 deformations explicitly by turning on a, b, c, d .

It immediately follows that \mathcal{T} deforms to \mathcal{E} , where

$$\mathcal{E}|_C = \begin{cases} \mathcal{O}(2) \oplus \mathcal{O}(-1) \oplus \mathcal{O}(-1) & \text{if } a = b = c = d = 0, \\ \mathcal{O}(1) \oplus \mathcal{O} \oplus \mathcal{O}(-1) & \text{if otherwise and } ad - bc = 0, \\ \mathcal{O} \oplus \mathcal{O} \oplus \mathcal{O} & \text{otherwise.} \end{cases} \tag{33}$$

There is therefore good news and bad news. The good news is that for a *generic* value of a, b, c, d we do indeed get a trivially split bundle and so instanton corrections prevent this being a good conformal field theory. The bad news is that we are left with a 3-dimensional space $ad - bc = 0$ where the bundle splits nontrivially. So we only removed one of our 4 spurious deformations.

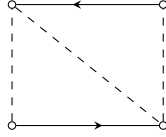


Figure 8: Minimal arrows for a $(-1, -1)$ -curve instanton.

4.4.2 Other Hilbert Scheme Deviations

The analysis of the previous section applies to any $(-1, -1)$ -curve. We get a very similar result in the case of complimentary defects as in figure 5. For every 4 obstructions we would like to obtain, we only get one.

In order to switch on Ext's to make the bundle trivially split we need to make $ad - bc \neq 0$. Thus we need, at a minimum, arrows of the form of figure 8. This provides a serious problem for the larger “minimal” defects as in figure 6. We are unable to get any instanton obstructions whatsoever from irreducible $(-1, -1)$ -curves.

4.4.3 The \mathbb{Z}_{11} case

Looking at figure 2 we see a similar picture. We take each of the five pictures in turn from top left to bottom right:

1. This is the Hilbert scheme.
2. At first sight the single $(-1, -1)$ -curve looks similar to the case of the previous section. However, the arrows are not oriented correctly. In particular node 6 has arrows only pointing away from it. This means the $\mathcal{O}(-1)$ associated to node 6 can never be turned into \mathcal{O} . Thus we get no instanton corrections, as expected.
3. The $(-1, -1)$ curve joining nodes 4 and 8 gives instantons. One of the 4 arrows is missing compared to section 4.4.1 so we set $d = 0$. So we have no instanton corrections if $bc = 0$. This is a codimension one condition, i.e., this instanton only obstructs one deformation. We were hoping to obstruct $41 - 39 = 2$.
4. The $(-1, -1)$ -curve joining nodes 1 and 5 is very similar to section 4.4.1. We expect to kill 4 deformations but the $ad - bc = 0$ condition results in only one deformation being lost.
5. The $(-1, -1)$ -curve joining nodes 3 and 8 is again very similar to section 4.4.1. So now we expect to kill 6 deformations but only end up killing one.

The result is that in the last three cases we do not kill enough deformations for geometry to agree with conformal field theory.

5 Other Sources of Instantons

5.1 Non-isolated toric curves

We now turn our attention to rational curves other than $(-1, -1)$ -curves. In general there will be more right-moving zero modes and left-moving zero modes. That is, we have a fermionic part of the instanton moduli space over which we must integrate.

This fermionic integration is familiar from topological field theory [4, 26] associated to the $N = (2, 2)$ case. In this σ -model, there is a term in the action given by

$$R_{i\bar{i}j\bar{j}}\lambda^i\bar{\lambda}^{\bar{i}}\psi^j\bar{\psi}^{\bar{j}}, \quad (34)$$

where λ and ψ are the left and right-moving fermions respectively, and $R_{i\bar{i}j\bar{j}}$ is the Riemann curvature of the Calabi–Yau X . The integrand over the supermoduli space contains the exponential of the action and thus any power of (34) appears. This allows an instanton contribution from any extra even number of ψ zero-modes so long as there is an equal number of extra λ zero-modes. In the topological field theory case, something very beautiful happens. These powers of the Riemann curvature tensor conspire to form the top Chern class which can be integrated over the the moduli space to form the Euler characteristic of the moduli space.

In the $(0, 2)$ case we replace the Riemann curvature tensor with the curvature of the bundle V , but in this paper we can put $V \cong \mathcal{T}$ to first order anyway. However, we cannot expect things to be as nice as the topological field theory case and should not expect to get characteristic classes. In this paper we will not attempt to do the instanton moduli space integration. We will just count fermion zero modes to account for the *possibility* of instanton corrections.

Let C have normal bundle $\mathcal{O}(-1 - m) \oplus \mathcal{O}(-1 + m)$. There are thus $2 + |m + 1| + |m - 1|$ right-moving fermion zero modes. To obtain a nonzero instanton correction to the destabilizing one-point function we need four more right-moving modes than left-moving modes. Thus we need $|m + 1| + |m - 1| - 2$ left-moving zero modes.

So, in the case $m = 0$ or $m = 1$ we need $V|_C$ to split trivially again. In the case $m \geq 2$ we need $V|_C$ to be split “more trivially” than the tangent bundle without actually splitting trivially. We show that there is actually only one possible splitting type for each m .

Proposition 5 *Let C have normal bundle $\mathcal{O}(-1 - m) \oplus \mathcal{O}(-1 + m)$, with $m > 0$. Then the number of fermion zero modes will force the instanton corrections to vacuum stability to vanish unless*

$$V|_C = \mathcal{O} \oplus \mathcal{O}(1 - m) \oplus (-1 + m). \quad (35)$$

If $m > 0$ then C itself contributes to the tangent bundle deformation count. Instead of

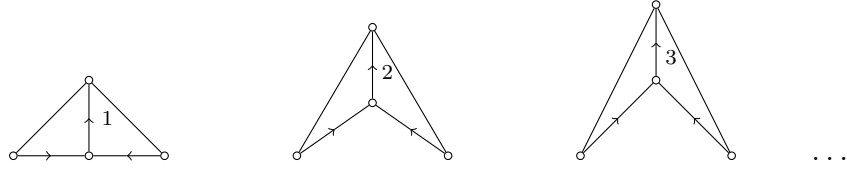


Figure 9: Configurations for non-isolated curves for $m = 1, 2, 3, \dots$

(31) we now have

$$\begin{array}{c}
 \mathcal{O}(1) \\
 \oplus \\
 \mathcal{O}(1) \\
 \oplus \\
 \mathcal{O}(-1-m) \\
 \oplus \\
 \mathcal{O}(-1+m)
 \end{array}
 \xrightarrow{\begin{pmatrix} x \\ y \\ 0 \\ 0 \end{pmatrix}}
 \mathcal{T}|_C \longrightarrow 0.
 \tag{36}$$

The diagram shows a sequence of maps. On the left, a map from 0 to \mathcal{O} is shown. This is followed by a map from \mathcal{O} to a direct sum of sheaves: $\mathcal{O}(1) \oplus \mathcal{O}(1) \oplus \mathcal{O}(-1-m) \oplus \mathcal{O}(-1+m)$. The map from \mathcal{O} to the direct sum is labeled with a column vector $\begin{pmatrix} x \\ y \\ 0 \\ 0 \end{pmatrix}$. Dotted arrows point from the top two $\mathcal{O}(1)$ terms to the $\mathcal{O}(-1-m)$ term. A double arrow points from the $\mathcal{O}(-1-m)$ term to the $\mathcal{O}(-1+m)$ term. Finally, a map from the direct sum to $\mathcal{T}|_C$ is shown, which then maps to 0 .

The double arrow shows the Ext's of dimension m that C itself is producing. Note, however, that this arrow is pointing in the wrong direction to restrict to anything nonzero on C . We show by dotted arrows the Ext's possibly contributed by intersecting curves that deform $\mathcal{T}|_C$. Using the methods of section 4.4.1 and the appendix, one can (eventually) show that turning both of these Ext's on gives (35). This is as close to trivial splitting as we can get, and happens to give exactly the $2m - 2$ zero modes needed above. ■

It follows that we get instanton corrections if subdiagrams of the form in figure 9 appear in our toric diagram. This is certainly possible in some examples. However, we have the following:

Proposition 6 *The Hilbert scheme resolution of \mathbb{C}^3/G has no worldsheet instanton corrections to $(0,2)$ -deformations coming from irreducible toric rational curves.*

To prove this note that it is impossible for any of the diagrams in figure 9 to appear. This follows from property 1 in proposition 1. That is, any arrow for the Hilbert scheme can be followed along a straight line until it reaches an outer vertex. This is clearly not compatible with figure 9.

The diagram in figure 8 is also not possible in the Hilbert scheme, since dotted lines only come from subdividing equilateral triangles, and so there are no corrections from $(-1, -1)$ -curves. ■

Returning to our examples, an examination of figure 2 shows that we never get diagrams of the form in figure 9 in the \mathbb{Z}_{11} case. Nor do they occur in the simple defect in figure 4. So these non-isolated curves do not resolve our discrepancies.

5.2 Reducible Curves

Rational curves minimize the action in a homotopy class of maps from S^2 into X . Unfortunately there is no promise that such a rational curve is smooth. A nodal rational curve might look like two rational curves intersecting transversely at a point, i.e., it is reducible. We must consider such cases as possible instantons.

The problem is that such a rational curve cannot be the image of a holomorphic map $\pi : \mathbb{P}^1 \rightarrow X$. To see this note that the inverse image of one of the components of the target rational curve would need to be a Zariski closed proper subset of \mathbb{P}^1 , but the only such subsets are points. This means the earlier analysis of this paper doesn't really apply. One possible solution is to consider smooth non-toric curves in the same family. We cover this in the next section.

The appearance of such nodal curves is very common in the above examples. For example, in the last diagram in figure 2 we can take the union $C_{38} \cup C_{48}$. Indeed, any time two rational curves meet at a point, we can take their union.

5.3 Multiple Covers

Another possibility is that the worldsheet map $\phi : \Sigma \rightarrow C$ is a multiple cover. Such maps are very important in the $N = (2, 2)$ case and there is no reason to suspect they will not have important effects in the $(0, 2)$ case as well. However, since we are no longer doing topological field theory, one would not expect such multiple covers to be given by the same Euler characteristic as in Gromov–Witten theory [4].

Unfortunately, fermion zero mode counting actually suggests more instanton corrections that we need. Consider a $(-1, -1)$ -curve C such that

$$V|_C = \mathcal{O} \oplus \mathcal{O}(-1) \oplus \mathcal{O}(1). \tag{37}$$

For this embedding, there are 4 right-moving zero modes (from $\mathcal{T}|_V$) and 2 left-moving modes.

If ϕ is a double cover, then the degree of each line bundle doubles. Thus $\phi^{-1}V = \mathcal{O} \oplus \mathcal{O}(-2) \oplus \mathcal{O}(2)$. We now have 8 right-moving and 4 left-moving zero modes. This has a difference of 4 and thus we might naïvely expect instanton corrections.

This is not good. The Hilbert scheme has many tangent bundle deformations leading to the split (37) and we don't want to obstruct these. Since we have merely counted zero modes, we haven't proven there actually are instanton corrections. Clearly there is more to be investigated here. In particular, one should try to understand the integral over the moduli space in analogy with [4].

5.4 Non-toric curves

We can also consider rational curves which are not toric. However, all rational curves are actually “seen” by toric rational curves in the following sense. There is a $(\mathbb{C}^*)^d$ -action on X . If a curve is completely fixed by this action then it is toric. If not, then the curve must

move in a family under this action. We can then take a limit of generic one-parameter subfamily of $(\mathbb{C}^*)^d$ to include the origin. The limit will then be a (not necessarily smooth) toric rational curve. Thus every rational curve is contained in a family including a toric rational curve.

A corollary of this statement is that an isolated rational curve must be toric. That is, all $(-1, -1)$ curves are toric. Thus we have already studied all instantons given by irreducible isolated rational curves.

Let us illustrate what can happen with an example in the \mathbb{Z}_{11} resolution appearing last in figure 2 (with 45 total deformations). The two monomials $x_1x_2^2x_6x_8$ and $x_3^2x_4$ have the same $(\mathbb{C}^*)^5$ -charge. Thus we may consider the homogeneous ideal $\mathcal{I}_{[\alpha,\beta]} = \langle \alpha x_1x_2^2x_6x_8 + \beta x_3^2x_4, x_7 \rangle$, for $[\alpha, \beta]$ some point in \mathbb{P}^1 . The irrelevant ideal for the case we are considering says that x_2, x_6, x_4 cannot vanish when $x_7 = 0$ so the above simplifies to

$$\mathcal{I}_{[\alpha,\beta]} = \langle \alpha x_1x_8 + \beta x_3^2, x_7 \rangle. \quad (38)$$

The divisor $x_7 = 0$ is isomorphic to \mathbb{P}^2 with homogeneous coordinates $[x_1, x_3, x_8]$, so this ideal is the ideal of a plane conic rational curve, which is smooth if α and β are nonzero.

Let $[u, v]$ be homogeneous coordinates on C and put $x_1 = \beta u^2, x_3 = -\alpha^{\frac{1}{2}}uv, x_8 = v^2$ to embed C into X . The restriction of the tangent sheaf to C is now given by

$$0 \longrightarrow \mathcal{O} \xrightarrow{\begin{pmatrix} u^2 \\ uv \\ v^2 \\ 0 \end{pmatrix}} \mathcal{O}(2)^{\oplus 3} \oplus \mathcal{O}(-6) \longrightarrow \mathcal{T}|_C \longrightarrow 0. \quad (39)$$

This gives $\mathcal{T}|_C \cong \mathcal{O}(3) \oplus \mathcal{O}(3) \oplus \mathcal{O}(-6)$ and so the adjunction (14) does not split. Indeed, any plane curve of degree > 1 will have such a non-splitting [27].

In this example, none of the deformations of \mathcal{T} do anything to this restriction, so this curve is certainly not a new source of instanton corrections.

Going to a generic toric limit is easy when given the corresponding ideal. One simply replaces any non-monomial generator by one of its monomials. Thus we have $\langle x_1x_8, x_7 \rangle$ or $\langle x_3^2, x_7 \rangle$. This corresponds to a reducible rational curve and a double cover respectively. Thus we see that the the reducible case and multiple covers are really aspects of the non-toric curve picture.

It is worth pointing out, however, that not every reducible rational curve is a limit of a family of smooth ones. Consider the union of C_{38} and C_{48} in the last diagram in figure 2 again. Within the surface $x_8 = 0$, these curves have self-intersection -1 and -2 respectively, and mutual intersection number 1. Thus, their union has self-intersection $-1 + 2 - 2 = -1$. Thus, a smooth curve in the same family would be a $(-1, -1)$ -curve, but this must be isolated which is a contradiction. Therefore $C_{38} \cup C_{48}$ cannot appear as the toric limit of a smooth family.

6 Discussion

We have had modest success in considering the effects of smooth toric rational curves. In the case of Hilbert schemes, where we do not need any instanton corrections, we do not get any. Furthermore, in examples we considered where we needed instanton corrections we frequently got some. The only problem is that the instantons we analyzed did not reduce the moduli space by enough dimensions to agree with conformal field theory.

Clearly there is a need to understand instantons on reducible rational curves. We suspect that these are the source of the discrepancies we find. Another direction which should be pursued is an analysis of the integration over moduli space required to understand multiple covers.

Acknowledgments

We thank R. Plesser for useful discussions. This work was partially supported by NSF grants DMS-0905923 and DMS-1207708. Any opinions, findings, and conclusions or recommendations expressed in this material are those of the authors and do not necessarily reflect the views of the National Science Foundation.

Appendix: Extensions on \mathbb{P}^1

In this appendix we review extensions of line bundles on \mathbb{P}^1 , which are central to this paper. Let \mathcal{E} satisfy

$$0 \longrightarrow \mathcal{O}(-n) \longrightarrow \mathcal{E} \longrightarrow \mathcal{O}(n) \longrightarrow 0. \quad (40)$$

Then what are the allowed sheaves \mathcal{E} ? The answer is

$$\mathcal{O}(-n) \oplus \mathcal{O}(n), \text{ or } \mathcal{O}(-n+1) \oplus \mathcal{O}(n-1), \dots, \text{ or } \mathcal{O} \oplus \mathcal{O}. \quad (41)$$

The first in this list is the trivial extension. In the space of possible extensions, we want to show that these extensions get more and more likely as we go down the list in the sense that they occupy a higher-dimensional set. The generic extension will then be the “trivial” split $\mathcal{O} \oplus \mathcal{O}$.

The space of extensions is given by

$$\text{Ext}^1(\mathcal{O}(n), \mathcal{O}(-n)) = H^1(\mathbb{P}^1, \mathcal{O}(-2n)) = \mathbb{C}^{2n-1}, \quad (42)$$

but we need to find exactly which extensions elements of this extension group give. We do this in the language of the derived category (or one could use push-out diagrams as in page 77 of [28].) The result is easy to state. If $f : \mathcal{O}(n)[-1] \rightarrow \mathcal{O}(-n)$ represents an element of $\text{Ext}^1(\mathcal{O}(n), \mathcal{O}(-n))$, then the desired extension \mathcal{E} is simply the mapping cone of f . The only work required is to explicitly relate this mapping cone to the possibilities listed in (41). Rather than doing this in generality we analyze the case $n = 2$. The same methods can be employed for any n .

Since

$$0 \longrightarrow \mathcal{O} \xrightarrow{\begin{pmatrix} x \\ y \end{pmatrix}} \mathcal{O}(1)^{\oplus 2} \xrightarrow{\begin{pmatrix} -y & x \end{pmatrix}} \mathcal{O}(2) \longrightarrow 0, \quad (43)$$

we have an isomorphism in $\mathbf{D}(\mathbb{P}^1)$ between $\mathcal{O}(2)$ and the complex given by the two left terms above. We may now apply $\otimes \mathcal{O}(-1)$ to (43) to get an isomorphism between $\mathcal{O}(1)$ and the complex $\mathcal{O}(-1) \rightarrow \mathcal{O}^{\oplus 2}$. Using this to eliminate $\mathcal{O}(1)$ and then using Gaussian elimination to find a minimal presentation we get a short exact sequence

$$0 \longrightarrow \mathcal{O}(-1)^{\oplus 2} \xrightarrow{\begin{pmatrix} x & 0 \\ y & x \\ 0 & y \end{pmatrix}} \mathcal{O}^{\oplus 3} \longrightarrow \mathcal{O}(2) \longrightarrow 0. \quad (44)$$

Repeating this process we get

$$0 \longrightarrow \mathcal{O}(-2)^{\oplus 3} \xrightarrow{\begin{pmatrix} x & 0 & 0 \\ y & x & 0 \\ 0 & y & x \\ 0 & 0 & y \end{pmatrix}} \mathcal{O}(-1)^{\oplus 4} \longrightarrow \mathcal{O}(2) \longrightarrow 0. \quad (45)$$

This isomorphism between $\mathcal{O}(2)$ and the complex given by the two left terms above allows us to explicitly see the required map f . The result is that \mathcal{E} is given by

$$0 \longrightarrow \mathcal{O}(-2)^{\oplus 3} \xrightarrow{\begin{pmatrix} a & b & c \\ x & 0 & 0 \\ y & x & 0 \\ 0 & y & x \\ 0 & 0 & y \end{pmatrix}} \begin{matrix} \mathcal{O}(-2) \\ \oplus \\ \mathcal{O}(-1)^{\oplus 4} \end{matrix} \longrightarrow \mathcal{E} \longrightarrow 0, \quad (46)$$

where $(a, b, c) \in \text{Ext}^1(\mathcal{O}(2), \mathcal{O}(-2)) \cong \mathbb{C}^3$.

Now to determine which possibility we have, note that we can distinguish between them by computing $H^0(\mathcal{E}(-1))$. This, in turn we get from the long exact sequence of (46). We get the explicit map between $H^1(\mathcal{O}(-3)^{\oplus 3})$ and $H^1(\mathcal{O}(-3) \oplus \mathcal{O}(-2)^{\oplus 4})$ using monomials $x^\alpha y^\beta$, with $\alpha, \beta < 0$ to represent local cohomology. The result is that $H^0(\mathcal{E}(-1))$ is given by the kernel of the matrix

$$A = \begin{pmatrix} a & 0 & b & 0 & c & 0 \\ 0 & a & 0 & b & 0 & c \\ 1 & 0 & 0 & 0 & 0 & 0 \\ 0 & 1 & 1 & 0 & 0 & 0 \\ 0 & 0 & 0 & 1 & 1 & 0 \\ 0 & 0 & 0 & 0 & 0 & 1 \end{pmatrix}. \quad (47)$$

A has rank 4 if and only if $a = b = c = 0$, and determinant $b^2 - ac$. Thus we get the final result

$$\mathcal{E} = \begin{cases} \mathcal{O}(-2) \oplus \mathcal{O}(2) & \text{if } a = b = c = 0, \\ \mathcal{O}(-1) \oplus \mathcal{O}(1) & \text{if otherwise and } b^2 - ac = 0, \\ \mathcal{O} \oplus \mathcal{O} & \text{otherwise.} \end{cases} \quad (48)$$

As promised, $\mathcal{O} \oplus \mathcal{O}$ occurs generically. Furthermore $\mathcal{O}(-1) \oplus \mathcal{O}(1)$ happens in a codimension one subspace of $\text{Ext}^1(\mathcal{O}(2), \mathcal{O}(-2))$ and $\mathcal{O}(-2) \oplus \mathcal{O}(2)$ only occurs in codimension 3.

References

- [1] P. Candelas, X. C. de la Ossa, P. S. Green, and L. Parkes, *A Pair of Calabi–Yau Manifolds as an Exactly Soluble Superconformal Theory*, Nucl. Phys. **B359** (1991) 21–74.
- [2] X. Wen and E. Witten, *World Sheet Instantons and the Peccei-Quinn Symmetry*, Phys.Lett. **B166** (1986) 397.
- [3] M. Dine, N. Seiberg, X. G. Wen, and E. Witten, *Nonperturbative Effects on the String World-Sheet*, Nucl. Phys. **B278** (1986) 769–789, and Nucl. Phys. **B289** (1987) 319–363.
- [4] P. S. Aspinwall and D. R. Morrison, *Topological Field Theory and Rational Curves*, Commun. Math. Phys. **151** (1993) 245–262, hep-th/9110048.
- [5] D. A. Cox and S. Katz, *Mirror Symmetry and Algebraic Geometry*, Mathematical Surveys and Monographs **68**, AMS, 1999.
- [6] J. Distler, *Resurrecting $(2,0)$ Compactifications*, Phys. Lett. **188B** (1987) 431–436.
- [7] J. Distler and B. R. Greene, *Aspects of $(2,0)$ String Compactifications*, Nucl. Phys. **B304** (1988) 1–62.
- [8] E. Silverstein and E. Witten, *Criteria for conformal invariance of $(0,2)$ models*, Nucl. Phys. **B444** (1995) 161–190, hep-th/9503212.
- [9] C. Beasley and E. Witten, *Residues and world-sheet instantons*, JHEP **10** (2003) 065, hep-th/0304115.
- [10] P. S. Aspinwall and M. R. Plesser, *Elusive Worldsheets Instantons in Heterotic String Compactifications*, arXiv:1106.2998.
- [11] P. S. Aspinwall, *A McKay-Like Correspondence for $(0,2)$ -Deformations*, arXiv:1110.2524.
- [12] B. Gaines, *$(0,2)$ -Deformations and the Hilbert Scheme*, arXiv:1404.4291.
- [13] P. S. Aspinwall, I. V. Melnikov, and M. R. Plesser, *$(0,2)$ Elephants*, JHEP **1201** (2012) 060, arXiv:1008.2156.
- [14] P. Berglund, T. Hübsch, and L. Parkes, *Gauge Neutral Matter in Three Generation Superstring Compactifications*, Mod. Phys. Lett. **A5** (1990) 1485–1492.
- [15] D. A. Cox, *The Homogeneous Coordinate Ring of a Toric Variety*, J. Algebraic Geom. **4** (1995) 17–50, alg-geom/9210008.
- [16] I. M. Gelfand, M. M. Kapranov, and A. V. Zelevinski, *Discriminants, Resultants and Multidimensional Determinants*, Birkhäuser, 1994.

- [17] A. Craw and M. Reid, *How to Calculate A-Hilb \mathbb{C}^3* , in “Geometry of toric varieties”, Sémin. Congr. **6**, pages 129–154, Soc. Math. France, Paris, 2002, arXiv:math/9909085.
- [18] E. Witten, *World Sheet Corrections via D-Instantons*, JHEP **0002** (2000) 030, hep-th/9907041.
- [19] E. I. Buchbinder, R. Donagi, and B. A. Ovrut, *Superpotentials for Vector Bundle Moduli*, Nucl. Phys. **B653** (2003) 400–420, hep-th/0205190.
- [20] P. S. Aspinwall and D. R. Morrison, *Quivers from Matrix Factorizations*, Commun. Math. Phys. **313** (2012) 607–633, arXiv:1005.1042.
- [21] V. V. Batyrev and D. A. Cox, *On the Hodge Structure of Projective Hypersurfaces in Toric Varieties*, Duke Math. J **75** (1994) 293–338, arXiv:alg-geom/9306011.
- [22] G. Gonzales-Sprinberg and J. L. Verdier, *Construction géométrique de la correspondance de McKay*, Ann. Sci. École Norm. Sup. **16** (1983) 409–449.
- [23] J. McOrist and I. V. Melnikov, *Summing the Instantons in Half-Twisted Linear Sigma Models*, JHEP **02** (2009) 026, arXiv:0810.0012.
- [24] M. Kreuzer, J. McOrist, I. V. Melnikov, and M. R. Plesser, *$(0,2)$ Deformations of Linear Sigma Models*, JHEP **1107** (2011) 044, arXiv:1001.2104.
- [25] D. Eisenbud, M. Mustață, and M. Stillman, *Cohomology on Toric Varieties and Local Cohomology with Monomial Supports*, J. Symbolic Comput. **29** (2000) 583–600, arXiv:math/0001159.
- [26] E. Witten, *The N-Matrix Model and Gauged WZW Models*, Nucl. Phys. **B371** (1992) 191–245.
- [27] A. van de Ven, *A Property of Algebraic Varieties in Complex Projective Spaces*, in “Colloque Géom. Diff. Globale (Bruxelles, 1958)”, pages 151–152, Centre Belge Rech. Math., Louvain, 1959.
- [28] C. A. Weibel, *An Introduction to Homological Algebra*, Cambridge Stud. in Adv. Math. **38**, Cambridge, 1994.